Available online at www.sciencedirect.com
ScienceDirect
Journal of the European Ceramic Society 29 (2009) 603–610
www.elsevier.com/locate/jeurceramsoc

Stability of concentrated suspensions of Al_2O_3–SiO_2 measured by multiple light scattering

Olga Burgos-Montes *, Rodrigo Moreno

Instituto de Cerámica y Vidrio, CSIC, c/Kelsen 5, Campus Cantoblanco, 28049 Madrid, Spain

Received 19 March 2008; received in revised form 1 July 2008; accepted 17 July 2008
Available online 6 September 2008

Abstract

The stability of ceramic suspensions can be predicted by means of zeta potential and particle size measurements but a major problem is that most existing techniques make use of diluted suspensions so that the concentrated suspensions frequently used in shape forming of ceramics are out of range. The propagation of light through a concentrated suspension can be used to characterise its colloidal stability. This work aims to study the variations of the structure of concentrated ceramic suspensions maintained at rest by multiple light scattering (MLS). This technique allows us to obtain information about the agglomeration processes that take place during ageing, like particle migration and particle aggregation. The results are compared with those obtained using conventional techniques such as the predictive tests (e.g. zeta potential and rheological behaviour of fresh suspensions) and ageing studies measured by rheometry. For such purpose, aqueous suspensions of alumina and alumina/silica (used to produce mullite by reaction sintering) have been studied.

Keywords: Al_2O_3; SiO_2; Light Scattering; Suspensions; Rheology

1. Introduction

The manufacture of ceramic products needs careful control of the different processing steps in order to prevent defect formation and to develop the microstructure needed to obtain the desired properties. The defects introduced in any one step of the process are retained in the next one and can be present in the final material. Colloidal processing allows the control of the early steps of powder processing and its evolution during forming and consolidation steps.

Colloidal processing is based on the study and manipulation of the interparticle forces involved in the suspension in order to obtain dense particle-packing and uniform microstructures.[1–5] The main mechanisms of stabilisation are the electrostatic repulsion, based on the repulsive forces among the double layers developed around amphoteric particles immersed in a polar liquid, and the steric hindrance, in which polymers are adsorbed on the particle surfaces thus impeding the direct contact between them. A third mechanism arises from the combination of the other two, namely the electrosteric mechanism, due to the action of charged polymers (i.e. polyelectrolytes) which combine the steric barrier provided by the polymer at short separation distances with the electrostatic repulsion related to the charges at longer distances.

There is a broad body of work dealing with the role of different kinds of deflocculants, on the colloidal stability and the rheological properties of ceramic suspensions. All these studies have demonstrated the suitability of polyelectrolytes for the preparation of stable, concentrated suspensions. Among them, polyacrylic-based deflocculants are probably the most commonly employed.[6–8] In opposition to the numerous studies concerning the prediction of stability through zeta potential and/or rheological measurements, which can be referred to as predictive tests, the studies dealing with the stability of ceramic suspensions against time are much less frequent. The predictive methods are used to select the conditions for the preparation of a stable suspension but are not able to predict how much time these suspensions maintain stable. For doing this, other techniques are being used, mainly based on the measurement of the rheological behaviour after different ageing times or the evaluation of settling behaviour by visual inspection of the sedimentation front.[9,10] These testing procedures give useful information

* Corresponding author.
E-mail address: oburgos@icv.csic.es (O. Burgos-Montes).

0955-2219/$ – see front matter © 2008 Elsevier Ltd. All rights reserved.
doi:10.1016/j.jeurceramsoc.2008.07.044

about durability and evolution of the suspension, but may lead to contradictory results because rheological measurements are dynamic tests in which the sample is submitted to shear forces whereas in the other tests the sample is in equilibrium at rest. Moreover, these techniques provide a useful picture of the overall stability at a macroscopic scale but do not allow determining the mechanism through which destabilisation occurs on ageing. This requires the use of a specific technique able to determine the agglomeration kinetics of particles stored in a cell at rest. Most existing techniques make use of diluted suspensions so that the concentrated suspensions frequently used in shape forming of ceramics are out of range. The propagation of light through a concentrated suspension can be used to characterise its colloidal stability. Some years ago an analytical instrument has been developed that can register the variations of the structure of emulsions and suspensions by multiple light scattering (MLS).[11–13] This technique analyses the effect of a light source through the sample, and the transmitted and the backscattered light allows us to obtain information about the agglomeration processes that take place during ageing, like sedimentation, creaming and particle aggregation (coalescence, flocculation).

The present work describes the study of physical destabilisation of concentrated ceramic suspensions using the MLS technique. The results are compared with those obtained using conventional techniques such as the predictive tests (e.g. zeta potential and rheological behaviour of fresh suspensions) and ageing studies measured by rheometry. For such purpose, aqueous suspensions of alumina and alumina/silica (used to produce mullite by reaction sintering) have been studied.

2. Experimental

A commercial α-alumina (Condea HPA05, USA), with average particle size of 0.4 μm and specific surface area of 9 m^2/g, and a colloidal silica suspension (LEVASIL 200A/40%, Germany) containing 40 wt% particles with average size of 15 nm, specific surface area of 200 m^2/g and pH 9, were employed as starting materials.

Colloidal stability was first evaluated through predictive tests by measuring the zeta potential as a function of pH using the Laser Doppler Velocimetry technique (Zetasizer NanoZS, Malvern, UK). The samples were prepared to 0.1 g/l solid content in a solution of KCl 10^{-2} M to maintain constant the ionic strength. The pH was adjusted using HCl (10^{-1} M) and KOH (10^{-1} M). Suspensions were stirred for 20 h prior to measurements in order to reach surface equilibrium. An ammonium salt of a polyacrylic acid PAA (Duramax D3005, Rohm&Haas, PA, USA) was used as a polyelectrolyte to provide electrosteric stabilisation at moderate pH values. It is supplied as an aqueous solution with a concentration of 35 wt% of active matter and has pH 7–8 and density of 1.16 g/cm^3. Zeta potential measurements were performed for different dispersant contents in order to study the influence of this additive on the stability.

Three concentrated suspensions were prepared: an alumina suspension with 50 vol.% of solids, and two suspensions of alumina with addition of silica as a secondary phase for obtaining a mixture of 96.4/3.6 (v/v) alumina/silica (which is the composition needed to produce 10 vol.% mullite in an Al_2O_3 matrix). These suspensions were prepared in deionised water to total solid contents of 40 and 50 vol.% (including the water of the colloidal silica suspension) and adding the amount of dispersant optimized according to the zeta potential measurements. The suspensions were homogenised in an alumina jar mill for 6 h. The final suspensions were labelled as A50 for the alumina suspension with 50 vol.% solids and AS40 and AS50 for the alumina/silica suspensions with 40 and 50 vol.% of solids, respectively. The final pH of the obtained suspensions was 6–7 and it did not significantly change with time within the range of this study.

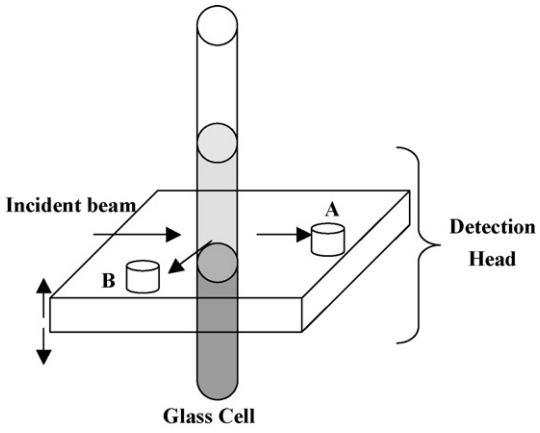

Fig. 1. Schematic representation of the MLS equipment, where A is the transmitted detector and B the backscattered detector.

The rheological behaviour of ball milled fresh suspensions was studied with a rheometer (RS50, Haake, Germany) using a double-cone/plate sensor configuration (DC60/2°, Haake, Germany). Two programs were employed: controlled rate (CR) and controlled stress (CS). CR program had three stages with a linear increase of shear rate from 0 to 1000 s^{-1} in 300 s, a plateau at 1000 s^{-1} for 120 s, and a further decrease to zero shear rate in 300 s. CS program had two stages with a linear increase of shear stress from 0 to 5 Pa in 120 s, and down to 0 in 120 s. Expanded viscosities curves were drawn by combining the data collected by both CS and CR tests. To study the ageing of the suspensions the viscosity curves were determined after 24 and 48 h, also. Suspensions were maintained under agitation with a low speed orbital shaker.

The physical destabilisation of the suspensions against time was evaluated by measuring the settling behaviour using the *multiple* light technique *scattering* (*MLS*) (Turbiscan Lab Expert, Formulaction, France) in which a pulsed near-infrared light source with a wavelength of 850 nm is forced to pass through a suspension maintained at rest into a glass tube. Fig. 1 shows a scheme of the MLS apparatus. It consists on a detection head that moves up and down along a glass cylindrical tube cell. It has a pulsed near-infrared light source (λ = 850 nm) and two synchronous optical sensors which receive the light transmitted through the sample (at 180° from the incident beam) and the light backscattered by the sample at 45° from the incident radiation, respectively. The detection head scans the entire length of the cell (by 65 mm) and takes data of transmission

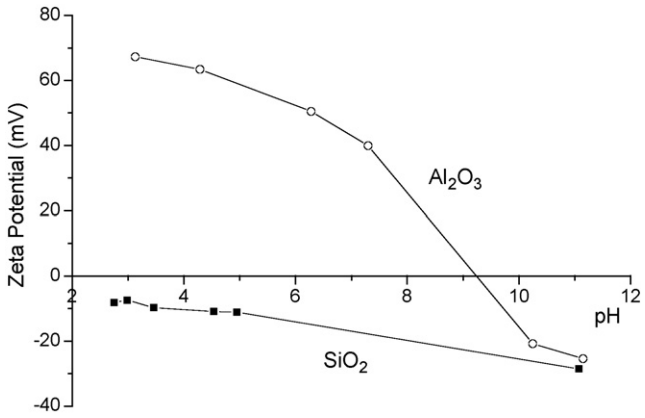

Fig. 2. Zeta potential versus pH of submicrometer-sized alumina and colloidal silica suspension.

and backscattering every 40 μm. A full description of the fundamentals and capabilities of this technique is given in Refs.[12,13] A major advantage of MLS as compared to other optical techniques such as microscopy, laser diffraction or dynamic light scattering, is that the former is non-destructive as no sample dilution is needed. The instrument is able to detect particle size variation or particle migration in concentrated and optical thick media. The amount of suspension needed for the MLS measurement is very low (4–8 ml). The equipment allows setting the number and the intervals for the scans. In this work the data were recorded every hour during 48 h, thus allowing studying the stability and the settling kinetics of the suspensions.

3. Results and discussion

3.1. Dispersion studies

The stability of alumina and silica suspensions was first studied by means of zeta potential measurements using the fresh suspension (time 0) at different pH values (Fig. 2). The zeta potential of colloidal silica is always negative and the absolute value slightly increases with pH. The alumina particles have an important dependence with pH, giving positive zeta potentials at acidic pH and negative ones at basic pH. The isoelectric point occurs by pH 9.0 as reported elsewhere for pure α-Al_2O_3.[14,15] For pH higher than 10 both the alumina and the silica particles have a negative charge and for lower pH the particles have opposite charge, which would lead to heterocoagulation.

In order to stabilise the mixture of alumina and silica at moderate pH, an ammonium salt of PAA was added as a dispersant. The variation of zeta potential of alumina and silica suspensions versus the concentration of dispersant is plotted in Fig. 3. On one hand, the addition of dispersant to alumina suspension provokes the change of sign of particles surface with a significant decease in the zeta potential values from +40 to −10 mV with the addition of only 0.2 wt%. Higher concentrations of dispersant make it change the zeta potential values to around −50 mV for 1.0 wt% and −60 mV for ≥1.2 wt%. On the other hand, the zeta potential of silica remains constant for any dispersant addition and it is considerably higher than that measured for silica without dispersant (around −40 mV). The optimum dispersant content for the mixture was considered to be 1.2 wt%, which is the concentration where a plateau is reached in the alumina curve. Zeta potential does not apparently depend on the solids content as this parameter accounts for the charges associated to individual particle surfaces. However, when solids content increases, separation distance among particles decreases and the interactions become stronger. In this case, although the zeta potential of suspensions with 0.8 wt% PAA is high enough to preserve stability, a higher content was selected (1.2 wt%) not only for the higher zeta potential, but also to increase surface coverage in order to avoid particles to touch each other. This concentration of deflocculant provides zeta potentials of −40 and −60 mV for silica and alumina, respectively, at the natural pH. Since the obtained pH is near neutrality (between 6 and 7) the addition of acids or bases was not considered as this could only difficult processing.

From these results, concentrated suspensions A50, AS50, AS40 were prepared adding 1.2 wt% of dispersant. At the obtained pH (∼8) both alumina and silica had negative surface charge allowing the electrostatic repulsion to have a key role in the stabilisation of the suspension. Fig. 4a shows the evolution of the viscosity with the shear rate for the fresh suspensions (the data of the CR and CS have been combined to obtain the expanded curve with data over five orders of magnitude). All the suspensions are stable and have moderate to low viscosity values, thus demonstrating that the dispersant content (1.2 wt%) selected according to zeta potential measurements is also adequate for the concentrated state. The highest viscosities were obtained for the A50 slurry. The mixture AS50 had a significantly lower viscosity although this slurry had the same volume fraction of solids as the A50 slip. Since there is no variation of pH and the zeta potential is always negative, a similar electrostatic repulsion is expected for both systems. The improved rheological behaviour of the mixture can be then related to the bimodal size distribution obtained when a secondary phase of colloidal silica is added to the coarse alumina particles. The reduction of viscosity in bimodal suspensions has been reported elsewhere.[16–18] Obviously, the viscosity of AS40 is lower as this slurry has a lower solid content.

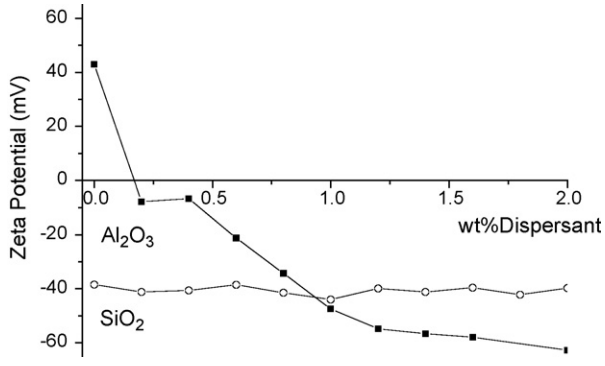

Fig. 3. Zeta potential versus concentration of PAA of alumina and colloidal silica suspensions.

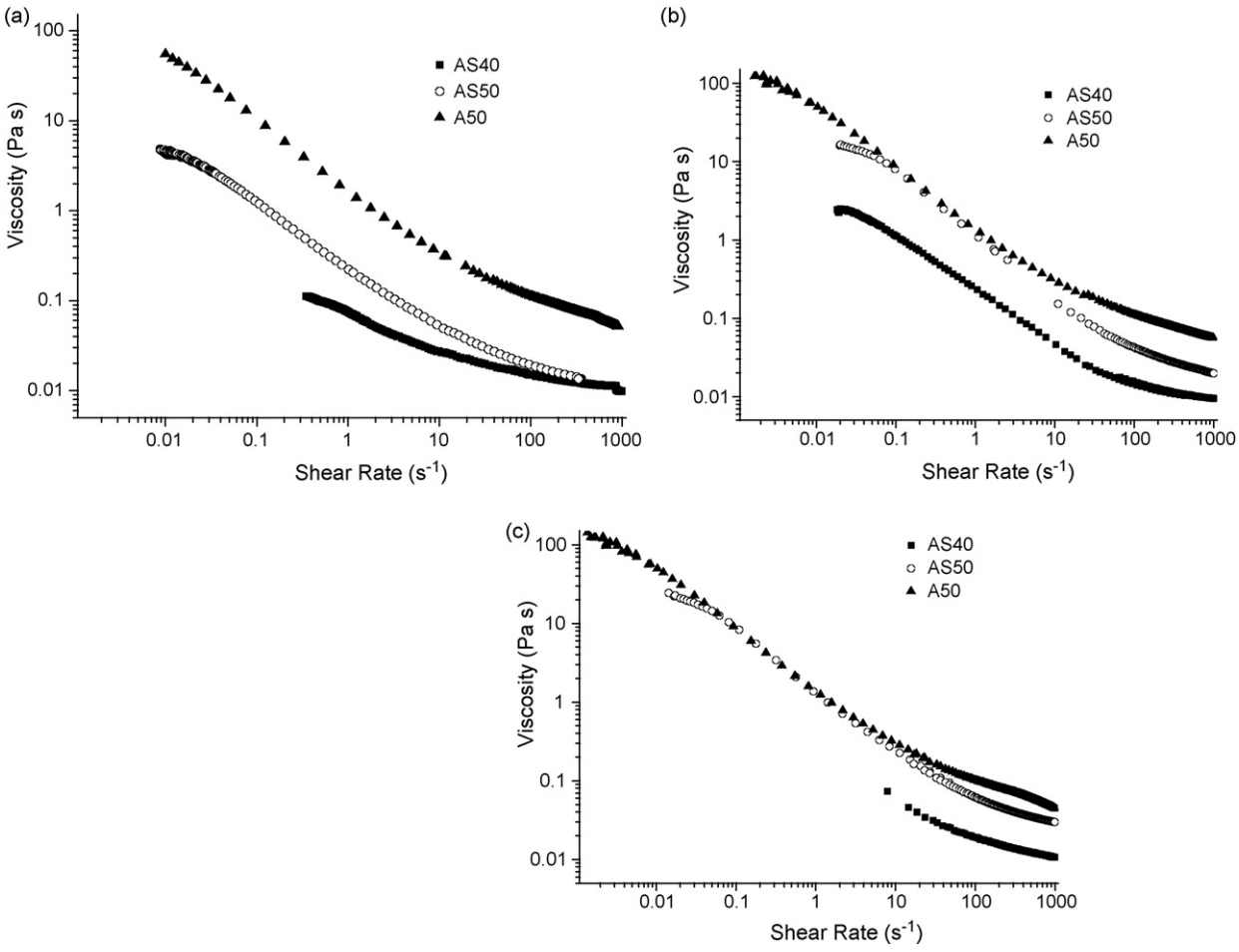

Fig. 4. Expanded viscosity curves of AS40, AS50 and A50 with 1.2 wt% of PAA for fresh suspensions (a), and after ageing for 24 h (b), and 48 h (c).

The curves plotted in Fig. 4 show a similar rheological behaviour in which viscosities tend to be constant at very low or very high shear rates, the so-called first and second Newtonian plateau, and have an intermediate zone where viscosity decreases as shear rate increases. This corresponds to a typical shear-thinning behaviour that considers that no yield point exists.[19–22] This is confirmed by the fact that the experimental data can be accurately fit using the Cross model for the viscosity:

$$\frac{\eta - \eta_\infty}{\eta_0 - \eta_\infty} = \frac{1}{1 + (K\dot{\gamma})^m} \quad (1)$$

where K is a constant and m is the power index. This is a 4-parameter model that considers the values of viscosity extrapolated to zero and infinite shear rate (η_0 and η_∞, respectively), which are reported in Table 1. The values of η_0 were obtained by extrapolation of the viscosity values measured at the low shear region in the CS curve whereas η_∞ values were obtained by extrapolating the high shear region values of the CR curves. The suspension A50 had the highest viscosity. When colloidal silica was added (AS50) the zero shear viscosity (η_0) was largely reduced from 160 to 6.5 Pa s. When the solids content was reduced to 40 vol.% (AS40) the viscosity decreased to 0.18 Pa s. The maximum difference between η_0 and η_∞ is less than three orders of magnitude, which is very low for the considered volume fraction of solids. The viscosity values and the rheological behaviour of the fresh suspensions reveal that they are homogeneous and well-dispersed.

Table 1
Values of the limit viscosities η_0 and η_∞ for the fresh A50, AS40, and AS50 suspension, and after 24, and 48 h ageing

	Fresh		24 h		48 h	
	η_0 (Pa s)	η_∞ (Pa s)	η_0 (Pa s)	η_∞ (Pa s)	η_0 (Pa s)	η_∞ (Pa s)
A50	160.3	0.054	199.4	0.032	145.5	0.011
AS50	6.30	0.010	19.39	0.018	32.3	0.023
AS40	0.18	0.008	3.17	0.008	1.211	0.0072

Table 2
Values of sedimentation rate for the fresh suspension and the suspension after 24 h of A50, AS40, and AS50

	U (cm/s)	
	Fresh	24 h
A50	8×10^{-6}	6×10^{-6}
AS50	2×10^{-4}	7×10^{-5}
AS40	9×10^{-3}	5×10^{-4}

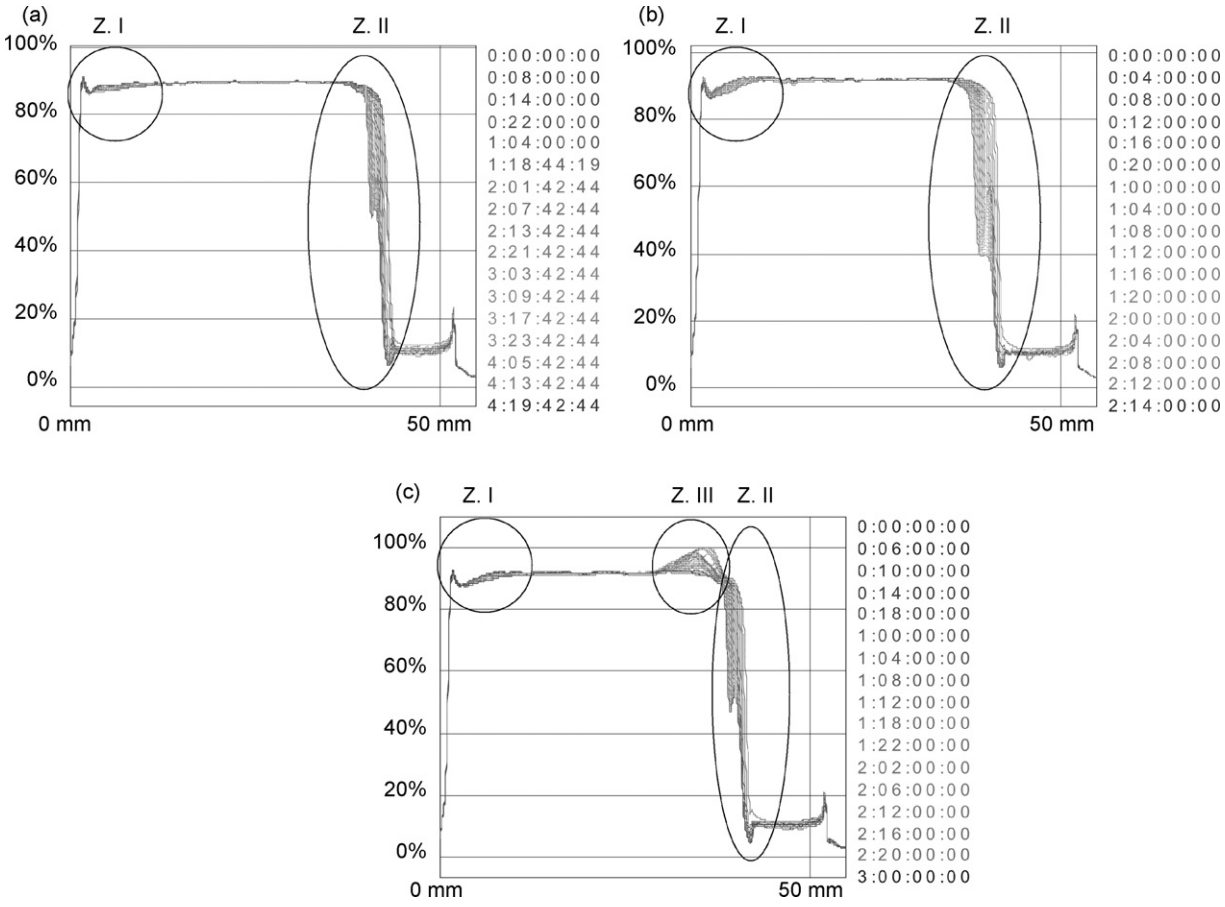

Fig. 5. Backscattered NIR light registered along the sample with time for A50 (a), AS40 (b), and AS50 (c).

3.2. Stability against time

The two major destabilisation phenomena are related to particle migration (creaming, sedimentation) and aggregation (coalescence, flocculation). Both of them have been studied using the MLS technique and aggregation has been studied by rheological measurements and particle size determinations. The theoretical sedimentation rate (U) is related to the viscosity by the Stokes' law:

$$U_S = \frac{2gd_{50}(\rho_p - \rho_f)}{9\eta_f} \quad (2)$$

where g is the acceleration due to gravity, d_{50} is the mean particle diameter, η_f is the viscosity of the fluid, and ρ_p and ρ_f are the densities of the particle and the fluid, respectively. Table 2 shows the sedimentation rate calculated for suspensions aged for 24 and 48 h, employing the η_0 values calculated for each one.[23] The highest sedimentation rate was obtained for the suspension AS40, just the one having the lowest solids loading (i.e. the lowest viscosity).[24]

The stability of the suspensions was first studied by measuring their rheological behaviour as prepared and after ageing for 24 and 48 h. Fig. 4b and c shows the expanded viscosity curves of the aged suspensions measured at the same conditions as used for the fresh suspensions. After 24 h (Fig. 4b), the viscosity of the suspensions has notably increased over that of the fresh suspensions. The highest viscosity corresponds to the suspension A50, followed by AS50, and the less viscous is the less concentrated AS40. This is clear when comparing the limit viscosities η_0 and η_∞ that are always higher for A50. However, at intermediate shear rates (between 0.1 and 10 s^{-1}) the viscosity of A50 and AS50 is the same. Although the sedimentation rate of the A50 suspension maintains constant, there is an important ageing effect in the alumina–silica suspensions and the sedimentation rate increases with longer ageing times (Table 2). The differences between the values of η_0 as a function of time are significant, especially for the bimodal suspension, η_∞ values being similar in all cases. So when the concentrated suspensions are under high shear stress, the suspensions recover their initial properties, being impossible to determine if some ageing process is occurring. Therefore it is necessary to employ another technique in order to predict and evaluate the ageing behaviour.

The influence of colloidal silica in the ageing of alumina suspensions was observed in previous work.[25] The viscosity curve after 48 h ageing shows a decrease in the viscosity, but this is due to the formation of a sediment at the bottom of the sample while the bulk suspension becomes less concentrated. Due to this lack of uniformity experimental viscosity data of these suspensions cannot be employed to calculate the sedimentation rate. The introduction of a colloidal fraction of silica makes the ageing behaviour to be different and time stability becomes shorter.

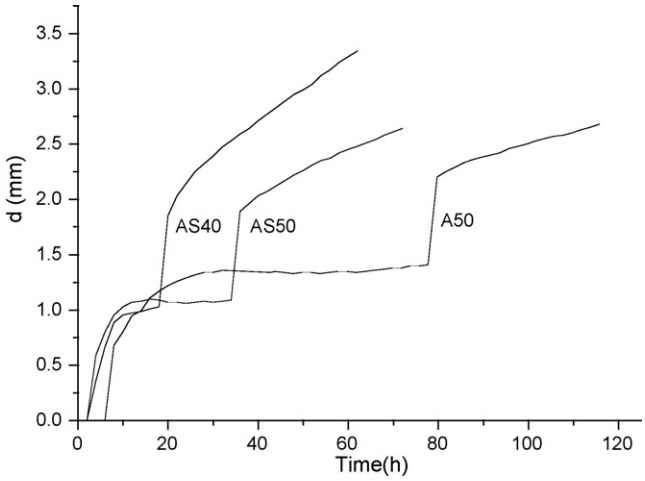

Fig. 6. Sedimentation kinetics of A50, AS40, and AS50 suspensions.

So far the stability of the suspension was evaluated by the zeta potential data and the viscosity of the suspensions in a broad range of shear rates. The possibility of determining the evolution of these suspensions with time in the stationary state could provide important additional information about the actual behaviour of the suspension, regarding the formation of a particle structure (i.e. the particle forces). During the MLS tests the transmission detector collects the light that passes through the sample and the backscattering one the backward scattered light. The concentrated suspensions: A50, AS50, and AS40 were introduced in the measuring cell and the backscattering and transmission signals were registered every hour up to 48 h. The suspensions are opaque due to the high solids content. The volume fraction (ϕ) of the concentrated suspensions is higher than the critical volume fraction (ϕ_c) therefore the transmission is close to zero.[11] For this reason only the backscattering data were analysed. Fig. 5 shows the evolution of the backscattering measurements through the cell every hour. In all cases there are two zones:

Zone I (in the bottom of the cell): The backscattering has a slight variation.
Zone II (in the top of the cell): The backscattering decreases with time due to the clarification of the suspension as settling takes place. In the early stages of the process it seems to be continuous. After several hours, the depletion in the graph could indicate the formation of a sedimentation front.

In the suspension AS50 (Fig. 5c) there is another feature, zone III (just below the sedimentation front, zone II). The backscattering increases and a broad peak is recorded that shifts toward the bottom of the cell with time.

The plateau observed in the graph is constant during the studied period indicating that aggregation phenomena are not taking place, so the particle size does not change.

The most representative zone in the sedimentation process is zone II, so that the data of the top are employed to establish the kinetics curves. Fig. 6 shows the evolution of the height of the sediment in the cell versus time, calculated from values of Fig. 5. The appearance of the curves is similar for all three suspensions. There are three segments: the first one corresponds to typical sedimentation process, this step being determined by the initial viscosity of the suspension (Stoke's law). The plateau found at the second part defines a stationary stage where the sedimentation front, due to the high solids content, is formed up to a critical point after which a quick sedimentation occurs. The time period of the stationary stage is related to the stability of the suspensions. The viscosity of the alumina–silica suspensions is always lower than that of the alumina suspension and thus, the sedimentation rate is higher (Eq. (2)). The gap of the sedimentation front occurs at 18, 35, and 78 h for AS40, AS50, and A50, respectively. These experimental data are in good agreement with the data calculated considering the Stoke's law (Table 2). However, the sedimentation rate after the gap is similar for all the suspensions. This effect is related to the ageing of the suspension.

Fig. 7 shows the evolution of the backscattered light versus time for the main zones of the cell. The backscattering in zone I is insignificant and the amount of particles is constant at the bottom of the cell. In zone II the curves show different segments: at the beginning there is a continuous decrease of backscattered light. In this zone alumina–silica suspensions have the same behaviour as A50 but the evolution of the backscattering is different, the slope of A50 being lower than that of the mixtures, this meaning that the sedimentation rate is also lower. In the final part of the curves the slope and the sedimentation rate decrease. The transition between the curves corresponds to the formation of the sedimentation front. At the cell top particles appear to sediment with a constant rate up to the formation of the sedimentation front; afterwards this sediment front moves slowly. For the suspension AS50 zone III is marked and shows an increase of the backscattering that indicates the accumulation of particles in this zone, just below the sedimentation front.

Fig. 8 shows a schematic representation of the particle arrangement in the suspensions at three different times: t_0 for the fresh suspension, t_1 in the first part of the curve where the sedimentation rate is faster, and t_2 in the final step of the process, as it is marked in Fig. 7. The suspensions AS40 and

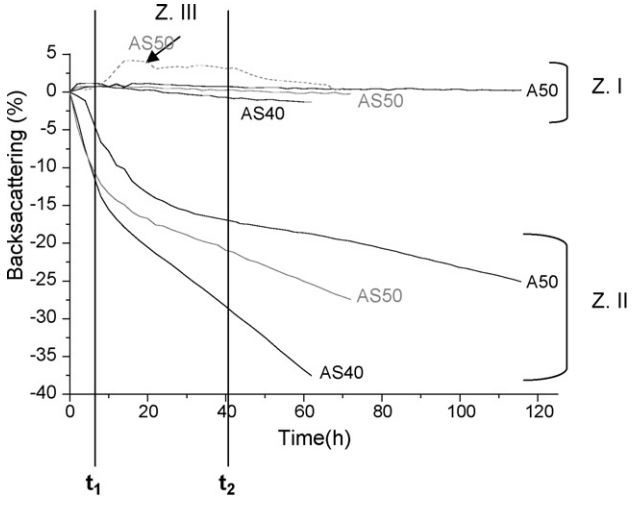

Fig. 7. Evolution of the backscattered NIR light with time.

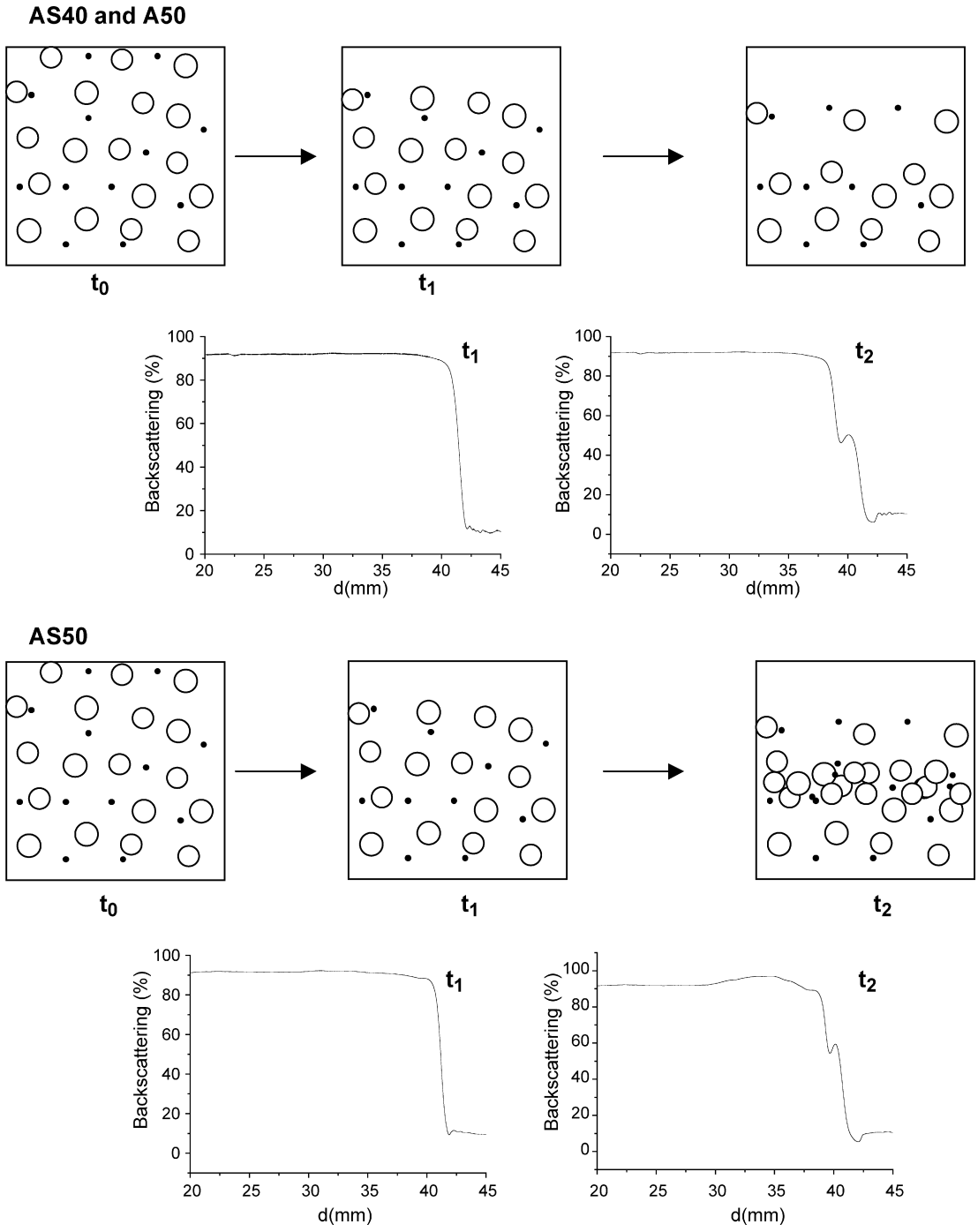

Fig. 8. Schematic representation of the particles behaviour during the destabilisation process.

A50 show a similar behaviour with the same stages, and AS50 has a different behaviour only in zone III, as it has been also observed in Fig. 6. For t_0, the particles in the fresh suspension are homogeneously dispersed. t_1 stands for the first step where the sedimentation rate is constant. A clear supernatant starts to appear in the top, and particles are uniformly distributed below. t_2 corresponds to the last step after the formation of the sedimentation front, where a section with particles (sedimentation front) can be distinguished in the clarification zone. The suspension AS50 has a slightly different behaviour due to the higher solids concentration and the presence of colloidal silica suspension as second phase. At the beginning the suspension is homogeneous along the whole cell and after several hours the clarification zone is detected. In the third step the clarification zone with the sedimentation front can be seen, similar to all the suspensions; however under this zone an increase in the backscattering is observed that corresponds to an accumulation of particles, losing the homogeneity of the suspension. Although the suspensions show similar rheological behaviour, the MLS a test allow a better characterisation of the concentrated suspensions, and permits to foresee the possibility of heterogeneities to appear through further shaping steps.

4. Conclusions

The dispersing conditions for alumina and alumina–silica suspensions were studied in terms of zeta potential and rheological behaviour. Stable suspensions were obtained adding 1.2 wt% (referred to dry solids) of an ammonium salt of PAA as a dispersant giving a zeta potential of −40 mV at moderate pH (6.5–7). The addition of the secondary silica phase to alumina produces a homogeneous packing of particles with a bimodal size distribution, reducing the viscosity of the suspension from 160 to 6.5 Pa s for A50 and AS50, respectively. However, whereas the alumina suspension remains constant within time the addition of the secondary silica phase provokes an important ageing effect.

The theoretical sedimentation rates (U) have been calculated from the limit viscosities. The highest sedimentation rate occurs for the suspension AS40, which has the lowest viscosity. The sedimentation kinetics of concentrated suspensions at rest was evaluated by MLS. Two main zones are observed in the cell: (I) the bottom, where backscattering has a slight variation and (II) the top of the cell, where clarification occurs due to settling. In the case of suspension AS50 there is a third zone (III) below the sedimentation front where particles accumulate and backscattering increases. The kinetics curves show a similar behaviour for all the suspensions. The sedimentation front occurs at 18, 35, and 78 h for AS40, AS50, and A50, respectively, which gives the limit for the stability against time. A schematic model is presented that illustrates how particles are homogeneously dispersed in the earlier stages, but after a certain time t_1 the sedimentation rate is constant and the clarification of the top begins. For a longer time t_2 the sedimentation front is formed inside the clarification zone, after which the sedimentation process continues. According to this, MLS technique is a promising tool giving useful information about the rheological behaviour of concentrated suspensions complementary to that obtained through rheological measurements, especially regarding the ageing evolution at rest. A further advantage over optical techniques such as those used measuring particle size distribution and zeta potential is that the MLS method is non-destructive and useful for concentrated, opaque suspensions.

Acknowledgement

This work has been supported by Spanish Ministry of Science and Innovation (Contract MAT2006-01038).

References

1. Lewis, J. A., Colloidal processing of ceramics. *J. Am. Ceram. Soc.*, 2000, **83**(10), 2341–2359.
2. Lange, F. F., Powder processing science and technology for increased reliability. *J. Am. Ceram. Soc.*, 1989, **72**(1), 3–15.
3. Sigmund, W. M., Bell, N. S. and Bergström, L., Novel powder-processing methods for advanced ceramics. *J. Am. Ceram. Soc.*, 2000, **83**(7), 1557–1574.
4. Hidber, P. C., Graule, T. J. and Gauckler, L. J., Influence of the dispersant structure on properties of electrostatically stabilized aqueous alumina suspensions. *J. Eur. Ceram. Soc.*, 1997, **17**(2–3), 239–249.
5. Moreno, R., The role of slip additives in tape casting technology. I. Solvents and dispersants. *Am. Ceram. Soc. Bull.*, 1992, **71**(10), 1521–1531.
6. Cesarano, J. and Aksay, I. A., Stability of aqueous α-Al_2O_3 suspensions with poly(methacrylic acid) polyelectrolyte. *J. Am. Ceram. Soc.*, 1988, **71**(4), 250–255.
7. Davies, J. and Binner, J. G. P., The role of ammonium polyacrylate in dispersing concentrated alumina suspensions. *J. Eur. Ceram. Soc.*, 2000, **80**(9), 2315–2325.
8. Hackley, V. A., Colloidal processing of silicon nitride with poly(acrylic acid). I. Adsorption and electrostatic interactions. *J. Am. Ceram. Soc.*, 1997, **71**(4), 250–255.
9. Bergström, L., Shear thinning and shear thickening of concentrated ceramic suspensions. *Colloid Surf. A*, 1998, **133**(1–2), 151–155.
10. Millán, A. J., Gutiérrez, C. A., Nieto, M. I. and Moreno, R., Aging behavior of alumina casting slips. *Am. Ceram. Soc. Bull.*, 2000, **79**(5), 64–68.
11. Buron, H., Mengual, O., Meunier, G., Cayré, I. and Snabre, P., Optical characterization of concentrated dispersions: applications to laboratory analyses and on-line process monitoring. *Polym. Int.*, 2004, **53**, 1205–1209 [Review].
12. Mengual, O., Meunier, G., Cayre, I., Puech, K. and Snabre, P., Turbiscan MA 2000: multiple light scattering measurement for concentrated emulsion and suspension instability analysis. *Talanta*, 1999, **50**(2), 445–456.
13. Mengual, O., Meunier, G., Cayre, I., Puech, K. and Snabre, P., Characterisation of instability of concentrated dispersions by a new optical analyser: the Turbiscan MA 1000. *Colloids Surf. A*, 1999, **152**(1–2), 111–123.
14. Tari, G., Ferreira, J. M. F. and Lyckfeldt, O., Influence of the stabilising mechanism and solid loading on slip casting of alumina. *J. Eur. Ceram. Soc.*, 1998, **18**(5), 479–486.
15. Anklekar, R. M., Borkar, S. A., Bhattacharjee, S., Page, C. H. and Chatterjee, A. K., Rheology of concentrated alumina suspension to improve the milling output in production of high purity alumina powder. *Colloids Surf. A*, 1998, **133**(1–2), 41–47.
16. Farris, R. J., Prediction of the viscosity of multimodal suspensions from unimodal viscosity data. *Trans. Soc. Rheol.*, 1968, **12**, 281–301.
17. Zhu, X., Jiang, D., Tan, S. and Zhang, Z., Dispersion properties of alumina powders in silica sol. *J. Eur. Ceram. Soc.*, 2001, **21**(16), 2879–2885.
18. Sánchez-Herencia, A. J., Hernández, N. and Moreno, R., Rheological behavior and slip casting of Al_2O_3–Ni aqueous suspensions. *J. Am. Ceram. Soc.*, 2006, **89**(6), 1890–1896.
19. Bergström, L., Rheology of concentrated suspensions. In *Surface and Colloid Chemistry, Advanced Processing*, ed. R. J. Pugh and L. Bergström. Marcel Dekker Inc., NY, USA, 1994, pp. 193–244.
20. Barnes, H. A., Hutton, J. F. and Walters, K., An introduction to rheology. *Rheology Series 3*. Elsevier Science Publishers B.V., Amsterdam, The Netherlands, 1989.
21. Moreno, R., Rheology. In *The Encyclopedia of Materials. Science and Technology. III. Structural Materials. Ceramic Processing*, ed. G. L. Messing. Elsevier Science, UK, 2001, pp. 8192–8197.
22. Moreno, R., *Reología de suspensiones cerámicas, Biblioteca de Ciencias, vol. 17*. CSIC, Madrid, Spain, 2005.
23. Chanamai, R. and McClements, D. J., Dependence of creaming and rheology of monodisperse oil-in-water emulsions on droplet size and concentration. *Colloids Surf. A*, 2000, **172**(1–3), 79–86.
24. Tseng, W. J. and Wu, C. H., Sedimentation, rheology and particle-packing structure of aqueous Al_2O_3 suspensions. *Ceram. Int.*, 2003, **29**(7), 821–828.
25. Burgos-Montes, O., Nieto, M. I. and Moreno, R., Mullite compacts obtained by colloidal filtration of alumina powders dispersed in colloidal silica suspensions. *Ceram. Int.*, 2007, **33**(3), 327–332.